

## Ambient vibration tests of XV century Renaissance Palace after 2012 Emilia earthquake in Northern Italy

Gian Paolo Cimellaro\* and Alessandro De Stefano<sup>a</sup>

*Department of Structural, Geotechnical and Building Engineering (DISEG), Politecnico di Torino, Torino, Italy*

*(Received March 11, 2014, Revised May 25, 2014, Accepted June 2, 2014)*

**Abstract.** This paper focuses on the dynamic behaviour of Mirandola City Hall (a XV century Renaissance Palace) that was severely damaged during May 2012 Emilia earthquake in Northern Italy. Experimental investigations have been carried out on this monumental building. Firstly, detailed investigations have been carried out to identify the identification of the geometry of the main constructional parts as well as the mechanical features of the constituting materials of the palace. Then, Ambient Vibration Tests (AVT) have been applied, for the detection of the main dynamic features. Three output-only identification methods have been compared: (i) the Frequency Domain Decomposition, (ii) the Random Decrement (RD) and the (iii) Eigensystem Realization Algorithm (ERA). The modal parameters of the Palace were difficult to be identified due to the severe structural damage; however the two bending modes in the perpendicular directions were identified. The comparison of the three experimental techniques showed a good agreement confirming the reliability of the three identification methods.

**Keywords:** structural health monitoring; output only methods; ambient vibration tests; historical buildings; earthquake damage; frequency domain decomposition; random decrement; Eigensystem Realization Algorithm; ERA; structural health diagnosis and prognosis

---

### 1. Introduction

The modal analysis techniques find greater application in engineering today. The advent of the modern computers allows the realization of complex finite elements models that are able to analyze the static and dynamic behaviour of the structures and their performances also in probabilistic terms (Cimellaro *et al.* 2011). However, it often happens that the dynamic behaviour calculated with a finite element analysis differ from that of a real structure; therefore modal updating is necessary through the comparison with experimental measurements. A common characteristic of all the structural identification methods is that they are non destructive techniques, and they can be applied both to new (e.g., in phase of testing) and existing (e.g., historical structures) structures.

Between the different structural identification methods in this paper we have decided to use the output-only methods because: (i) the tests are fast and economic, since no equipments are

---

\*Corresponding author, Assistant Professor, E-mail: [gianpaolo.cimellaro@polito.it](mailto:gianpaolo.cimellaro@polito.it)

<sup>a</sup> E-mail: [alessandro.destefano@polito.it](mailto:alessandro.destefano@polito.it)

necessary for exciting the structure; (ii) Measurements are taken in normal operating conditions, so the identified modal parameters are representative of the dynamic behaviour of the structure in normal operating conditions; (iii) the tests do not interfere with the functionality of the structure. Many examples of application of output-only methods can be found in the literature, such as Abdel-Ghaffar *et al.* (1985), Chang *et al.* (2001), Nagayama *et al.* (2005), Saudi *et al.* (2009), Piantà *et al.* (2011). Few full scales ambient vibration tests of historical monumental buildings that were damaged after earthquakes can be found in the literature, probably because of the inaccessibility right after an earthquake which severely damaged structures and because of the difficulty in identifying its dynamic behavior. Therefore this paper presents the experimental identification tests that were conducted on Mirandola Town Hall palace right after May 2012 Emilia earthquake.

## 2. Identification methods of modal parameters

In this paper three output only identification methods are compared. The first is a method that works in the frequency domain using the peak picking (PP) method (Brickler *et al.* 2000) and as the name suggests is based on the selection of the modal frequencies from the peaks of the output measurement spectra. The other two methods work in the time domain. The random decrement technique (RD) converts the output signals to free decays using the RD functions (Cole 1968).

The natural excitation technique (NExT) uses the auto and cross-correlation functions of output signals that are treated as sums of decaying sinusoids (James *et al.* 1993, 1996). Each decaying sinusoid has a frequency and damping ratio identical to that of a structural mode. Then, the modal identification techniques that use impulse responses as input such as eigensystem realization algorithm (ERA) can be used to extract the modal parameters from these free decays (Juang and Pappa 1985, 1986). Further details about the identification methods used in this paper can be found also in Cimellaro *et al.* (2012).

## 3. Frequency Domain Decomposition technique

The classical approach of *output-only modal identification methods* is based on a single signal processed using the Discrete Fourier Transform (DFT), where the peaks of the Power Spectral Density (PSD) matrix can be used to give reasonable estimates of natural frequencies and mode shapes if the modes are well separated. However, in the case of superimposed modes, it is difficult to identify the peaks of close modes and the frequency estimates are limited by the frequency resolution of the spectral density estimates. The *Frequency Domain Decomposition (FDD)* (Brincker *et al.* 2000) removes all the disadvantages associated with the classical approach, but keeps the important features of user-friendliness and even improves the physical understanding by dealing directly with the Spectral Density Function. The results of the FDD are exact when the input is a white noise, the structure is slightly damped and the modal forms of the coupled modes are orthogonal. If these hypotheses are not verified, the decomposition in SDOF systems is approximate; however, results are more accurate than those methods. In the FDD method, the first step is to estimate the PSD matrix. The estimate of the output PSD  $\mathbf{G}_{yy}(j\omega)$  known at discrete frequencies  $\omega = \omega_i$  is then decomposed by taking the Singular Value Decomposition (SVD)

of the matrix

$$\mathbf{G}_{yy}(j\omega_i) = \mathbf{U}_i \mathbf{S}_i \mathbf{U}_i^H \quad (1)$$

where the matrix  $\mathbf{U}_i = [\mathbf{u}_{i1}, \mathbf{u}_{i2}, \dots, \mathbf{u}_{in}]$  = unitary matrix of singular vectors  $\mathbf{u}_{ij}$ , and  $\mathbf{S}$  = diagonal matrix of scalar singular value  $s_{ij}$ . Assuming an  $n$  degree of freedom system, the  $n$  dominating peaks (singular values) of the auto Power Spectral Density function correspond to the mode shape  $\phi = \mathbf{u}_{i1}$  and they can be selected either manually or with some available techniques. The complete analytical formulation of the method can be found in Brincker *et al.* (2000).

#### 4. Random decrement identification method

The Random Decrement (RD) technique was proposed by Cole (1968) in the late sixties as part of his work at NASA concerning the analysis of the dynamic response of space structures subjected to ambient loads. First, the RD functions were interpreted as free vibration responses of a system. Later it was proved that, under the assumption that the analyzed responses are a realization of a zero mean stationary Gaussian stochastic process, the RD functions are proportional to the correlation functions of the responses and to their first derivatives with respect to time. The RD method is easy to understand if one thinks that the response of a system to random input loads at each time instant  $t$ , is composed of three parts: the response to an initial displacement, the response to an initial velocity and the response to the random input loads between the initial state and the time instant  $t$ . By averaging a large number of time segments of the response with the same initial condition, the random part of the response will have a tendency to disappear from the average, and what remains is the response of the system to the initial conditions. From this simple explanation, the interpretation of the RD functions as free vibration responses of a system is obvious.

#### 5. Eigensystem realization algorithm technique

The Eigensystem Realization Algorithm is a parametric method in the time domain that is used in combination with the Natural Excitation Technique (NExT). This technique was proposed in the early 1990s for modal identification from output-only measurements under natural excitation. The basic principle behind the NeXT is that the theoretical cross-correlation function between two response measurements made along two degrees of freedom (DOF) collected from an ambient (broad-band) excited structure has the same analytical form as the free vibration response of the structure. Once an estimate of the response cross-correlation vector is obtained for a given reference channel, the ERA method (Juang and Pappa 1985) can be used to extract the modal parameters. A key issue in the application of NExT is to select the reference channel away from the modal nodes in order to identify all the modes. The theoretical background of NeXT- ERA is reported below because it is also able to identify damping and an index (MAC) which describes the goodness of the results.

### 5.1 Theoretical background of the NExT

The NExT technique introduced by James *et al.* (1993, 1996), has been successfully used for identification of structures based on *output-only* information (Caicedo *et al.* 2004). The basic idea behind the NExT method is that the cross-correlation function, between the response vector and the response of a selected reference DOF, satisfies the homogeneous equation of motion, if the excitation and responses are weakly stationary random processes, which is normally the case for ambient vibration. Then, Equation of motion can be written as

$$\mathbf{M}E\left[\ddot{\mathbf{x}}(t) \mathbf{x}_{ref}(t-\tau)\right] + \mathbf{C}E\left[\dot{\mathbf{x}}(t) \mathbf{x}_{ref}(t-\tau)\right] + \mathbf{K}E\left[\mathbf{x}(t) \mathbf{x}_{ref}(t-\tau)\right] = E\left[\mathbf{f}(t) \mathbf{x}_{ref}(t-\tau)\right] \quad (2)$$

where  $\mathbf{x}$ ,  $\dot{\mathbf{x}}$ ,  $\ddot{\mathbf{x}}$  and  $\mathbf{f}$  are displacement, velocity, acceleration and excitation stochastic vector processes, respectively, and  $E[\ ]$  is the expectation operator. Considering the definition of the correlation function  $R(\cdot)$ , one can rewrite Eq. (2) as

$$\mathbf{M}R_{x_{ref}\ddot{x}}(\tau) + \mathbf{C}R_{x_{ref}\dot{x}}(\tau) + \mathbf{K}R_{x_{ref}x}(\tau) = R_{x_{ref}f}(\tau) \quad (3)$$

Since the excitation and the system responses are weakly stationary random processes, they are uncorrelated, therefore  $R_{x_{ref}f}(\tau) = 0$ . On the other hand, it can be proven that (Bendat and Piersol 2000)

$$R_{x_{ref}\dot{x}}(\tau) = \dot{R}_{x_{ref}x}(\tau), \quad R_{x_{ref}\ddot{x}}(\tau) = \ddot{R}_{x_{ref}x}(\tau) \quad (4)$$

Using the above mentioned results, Eq. (3) can be rewritten as

$$\mathbf{M}\ddot{R}_{x_{ref}x}(\tau) + \mathbf{C}\dot{R}_{x_{ref}x}(\tau) + \mathbf{K}R_{x_{ref}x}(\tau) = 0 \quad (5)$$

Eq. (5) indicates that the cross correlation function between the displacement process vector and the reference DOF displacement, satisfies the homogeneous (or free vibration) equation of motion. It can be similarly shown that the acceleration cross correlation function, also satisfies the homogeneous (or free vibration) equation of motion

$$\mathbf{M}\ddot{R}_{x_{ref}\ddot{x}}(\tau) + \mathbf{C}\dot{R}_{x_{ref}\ddot{x}}(\tau) + \mathbf{K}R_{x_{ref}\ddot{x}}(\tau) = 0 \quad (6)$$

Previous experience has shown that it not possible to rely on a single reference DOF for the identification of all the modes. The optimum accuracy for the identification of different modes typically occurs with different selections of the reference DOFs, therefore the identification algorithm should use multiple DOFs. The importance of Eq. (6) is that: (i) the stationary random excitation (ambient noise) is eliminated from the equation of motion, and that (ii) only the acceleration records are needed to implement the identification technique. Once the homogeneous Eq. (6) of motion is formed using the NExT technique, ERA can be used to extract the modal parameters of the homogeneous model.

### 5.2 Theoretical background of the ERA

Juang and Pappa (1985, 1986) proposed an Eigensystem Realization Algorithm (ERA) for modal parameter identification and modal reduction of linear dynamical systems. The first

fundamental step is to form the  $n(r+1) \times m(p+1)$  Hankel block data matrix as follows

$$\mathbf{H}(k-1) = \begin{bmatrix} \mathbf{Y}(k) & \mathbf{Y}(k+1) & \cdots & \mathbf{Y}(k+p) \\ \mathbf{Y}(k+1) & \mathbf{Y}(k+2) & \cdots & \mathbf{Y}(k+p+1) \\ \cdots & \cdots & \cdots & \cdots \\ \mathbf{Y}(k+r) & \mathbf{Y}(k+r+1) & \cdots & \mathbf{Y}(k+p+r) \end{bmatrix} \quad (7)$$

where  $n$  and  $m$  are the number of measurement stations, and reference DOFs, respectively;  $r$  and  $p$  are integers corresponding to the number of block rows and columns, respectively.  $\mathbf{Y}(k)$  is the  $n \times m$  matrix of the cross-correlation functions which satisfies the homogeneous equation of motion (Eqs. (22) and (23)), and can be written as:

$$\mathbf{Y}(k) = \begin{bmatrix} y_{1,1}(k) & y_{1,2}(k) & \cdots & y_{1,m}(k) \\ y_{2,1}(k) & y_{2,2}(k) & \cdots & y_{2,m}(k) \\ \cdots & \cdots & \cdots & \cdots \\ y_{n,1}(k) & y_{n,2}(k) & \cdots & y_{n,m}(k) \end{bmatrix} \quad (8)$$

Originally,  $y_{i,j}(k)$  was meant to be the impulse response of the  $i^{th}$  DOF, at time step  $k$ , due to an impulse input at the  $j^{th}$  DOF. Here, since the impulse responses are not available, they are replaced by cross-correlation function  $R_{x_{ref}\ddot{x}}(k)$  of DOF  $i$ , at time step  $k$ , due to the selection of reference DOF  $j$ . The formulation represented by Eq. (8), enables one to use multiple reference DOFs simultaneously. A similar approach for simultaneous use of multiple reference DOFs can be found in the work of He *et al.* (2006). The ERA process starts with factorization of the Hankel block data matrix, for  $k=1$ , using singular value decomposition

$$\mathbf{H}(0) = \mathbf{P} \mathbf{D} \mathbf{Q}^T = [\mathbf{P}_1 \quad \mathbf{P}_2] \begin{bmatrix} \mathbf{D}_1 & 0 \\ 0 & 0 \end{bmatrix} \begin{bmatrix} \mathbf{Q}_1^T \\ \mathbf{Q}_2^T \end{bmatrix} = \mathbf{P}_1 \mathbf{D}_1 \mathbf{Q}_1^T \quad (9)$$

where  $\mathbf{D}$  is the diagonal matrix of monotonically non-increasing singular values.  $\mathbf{D}_1$  is  $N \times N$  ( $N \leq p$ ) diagonal matrix formed by truncating the relatively small singular values, where  $N$  is the final system order. It is worth noting that the selection of the final model order is not a trivial task.  $\mathbf{P}_1$  and  $\mathbf{Q}_1$  are  $n \cdot (r+1) \times N$  and  $m \cdot (p+1) \times N$  matrices, that include the first  $N$  columns of the original  $\mathbf{P}$  and  $\mathbf{Q}$  matrices, respectively. The discrete-time state-space realization matrices for the structural model can be estimated (Juang and Pappa 1985) as

$$\begin{aligned} \mathbf{A} &= \mathbf{D}_1^{-1/2} \mathbf{P}_1^T \mathbf{H}(1) \mathbf{Q}_1 \mathbf{D}_1^{-1/2} \\ \mathbf{C} &= \mathbf{E}_m^T \mathbf{P}_1 \mathbf{D}_1^{1/2} \end{aligned} \quad (10)$$

where  $\mathbf{E}_m^T = [I \quad 0]$  and the size is determined accordingly. The control influence matrix cannot be estimated using the output-only information. The estimated discrete-time realization needs to be transformed to the continuous-time domain format. Let's consider the eigenvalue problem for  $\mathbf{A}$

$$\mathbf{A} = \boldsymbol{\Psi} \boldsymbol{\Lambda} \boldsymbol{\Psi}^{-1} \quad (11)$$

where  $\Lambda$  and  $\Psi$  are the eigenvalue and eigenvector matrices, respectively. The natural frequencies  $\omega_i$ , damping ratios  $\zeta_i$  and the mode shapes  $\Phi_i$  of the continuous-time structural model can be found as follows

$$\omega_i = \sqrt{\sigma_i^2 + \Omega_i^2}, \quad \zeta_i = -\cos[\tan^{-1}(\Omega_i / \sigma_i)], \quad \Phi_i = \mathbf{C} \Psi_i \quad (12)$$

where

$$\Lambda = \text{diag}(\bar{\sigma}_i \pm j\bar{\Omega}_i), \quad \sigma_i \pm j\Omega_i = \frac{\ln(\bar{\sigma}_i)}{\Delta t} \pm j \frac{\ln(\bar{\Omega}_i)}{\Delta t} \quad (13)$$

where  $\Delta t$  is the sampling period of data records. In order to reduce the bias error due to noise corruption in the measurement, an alternative form of the ERA, named ERA/DC was developed (Juang *et al.* 1988). With this technique, we also calculate the Modal Assurance Criterion (MAC) coefficient that can guess values from 0 to 100 and describes the goodness of the results. The identification of the single degree of freedom system is realized using the singular vector corresponding to the peak singular value and applying a correlation analysis based on the MAC criterion

$$\text{MAC}(\phi_r, \phi_i) = \frac{|\phi_r^H \phi_i|^2}{[\phi_r^H \phi_r] \cdot [\phi_i^H \phi_i]} \quad (14)$$

where:  $\Phi_r$  = reference singular vector and  $\Phi_i$  = singular vectors related to the singular values near the peak. After choosing a MAC value we proceed to the comparison. If in the comparison with the  $i^{\text{th}}$  vector we obtain a greater or equal MAC to the select level, then this vector is selected and the corresponding singular value contributes to the definition of the bell. It is clear that for lower values of the MAC index larger bells are obtained, but smaller precision in the identification of a single degree of freedom system.

## 6. Case study: structural description

A fifteen century masonry structure located in Mirandola, Italy that was damaged during May 20th, 2012 earthquake, has been used as the case study to compare the three identification methods (Cimellaro *et al.* 2012).

The Town Hall was built in 1468 while the South arcades were added in 1748. Finally the entire building was heavily restored in the late nineteenth century. The north arcades of the facade rests on elegant pink marble columns. Some of them report engraved units formerly in use in the Duchy of Mirandola. The Town Hall consists of three separate buildings which were constructed in three different phases: the northern part, which overlooks the square, in the Renaissance style dates back to 1468 and went to integrate an existing building, which most likely was the former Town Hall (Fig. 2).

The southern Tuscan arcade-style, by the engineer Angelo Mirandola Scarabelli-Pedoca was added to the core building in 1748, and followed the creation of today's Piazza Mazzini, which necessitated the demolition of the adjacent houses to make room for a porch for the trading of wheat. At the end of the nineteenth century heavy restructuring became necessary, with the total

demolition and restoration of the arcades designed by the architect Vincenzo Maestri of Modena (Fig. 1). In 1928-1930, the architect Mario Guerzoni reorganized the interior spaces of the building, planning the closure of the central courtyard by fitting inside a grand staircase inside. The Mirandola Town Hall has rectangular plan with dimensions of about 35.18 m × 27.00 m and has a height of 16.8 m (Fig. 2). The palace has been seriously damaged during May 20<sup>th</sup> 2012 earthquake.



Fig. 1 Mirandola Town Hall after temporary safety measures

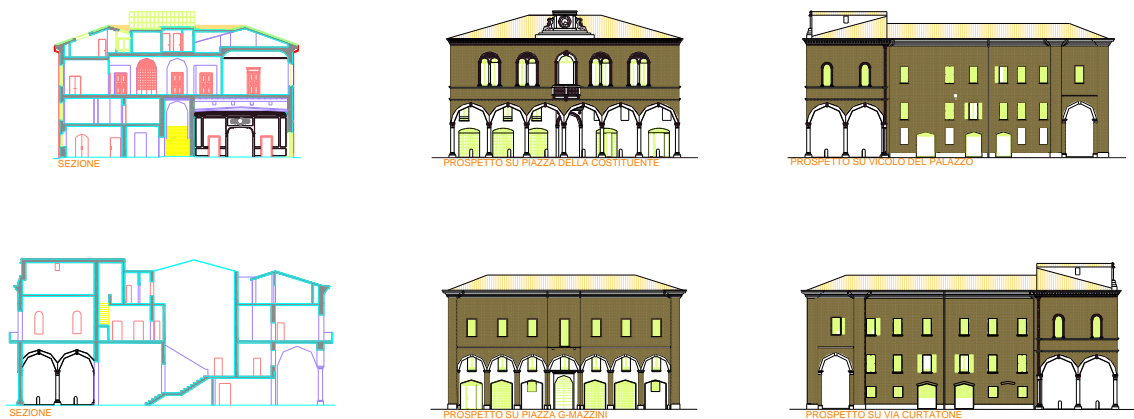


Fig. 2 Section and lateral view of the Palace

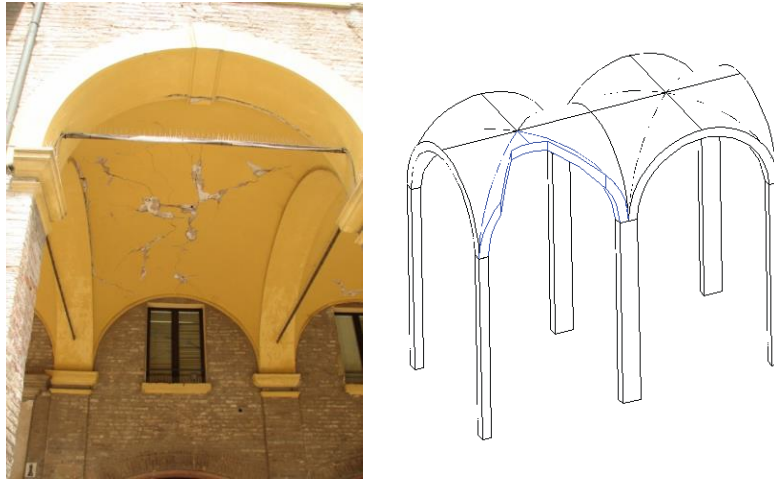


Fig. 3 Local collapse of the South vault

The main damage mechanisms detected during the field observations (Cimellaro *et al.* 2012) can be divided in two categories: (i) those related to the wall tilting caused by seismic forces agent orthogonal to the plan of the wall and (ii) those related to the formation of diagonal cracks caused by seismic forces parallel to the plan of the wall. The first mechanism is mainly visible on both the North and South external facades of the palace where it is possible to see of axial flexural failure of the pink marble columns of the North facade and pullout from the masonry wall of the wooden head beams supporting the first floor. This mechanism also initiated the local collapse of one of the vaults in the South facade (Fig. 3).

The second mechanism occurred below the external windows of the first floor on the west side and on the internal walls of the palace supporting the central staircase (Fig. 4).



Fig. 4 Diagonal cracks on external windows

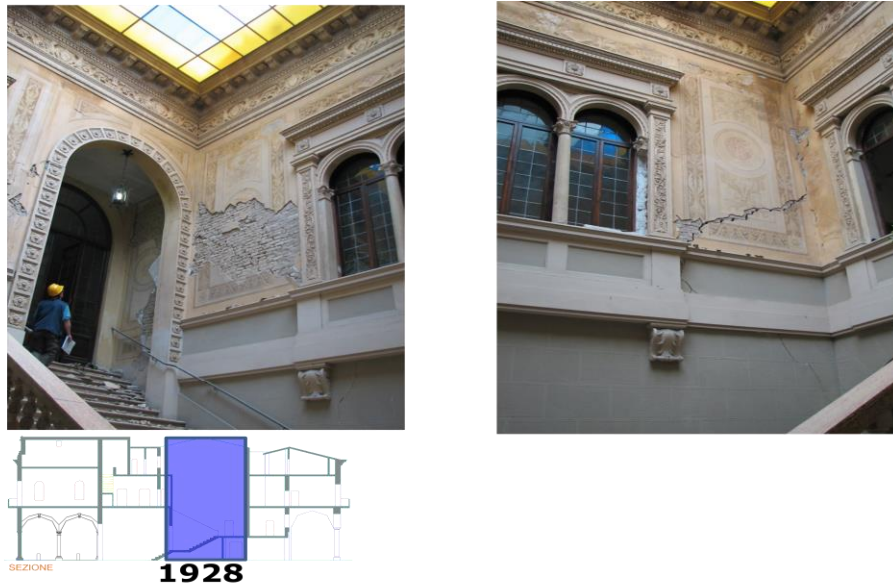


Fig. 5 Shear cracks in the main internal staircase

Additionally, there are other local damages that do not belong to the previous categories, like the shear cracks in the cross vaults of the south arcades, damage on the roof cover and damage that protude external element. Most of the internal damages and shear cracks concentrate near the central walls of the courtyard which are supporting the heavy and stiff central staircase (Fig. 5). Temporal emergency interventions with steel and wooden tubes for safety measuring were already set up at the moment of the test campaign both in the South, North and West facade (Fig. 1), but they did not interfere with the modal identification, because they were not activated by the low amplitude ambient vibrations.

## 7. Data acquisition system during identification tests

### 7.1 Instrumentation and sensors' configuration

21 accelerometers located according to the scheme shown in Fig. 6 and a data acquisition system located on the first floor (Fig. 7(a)) have been used for the data acquisition. The test campaign lasted one week and five different configurations were tested using 21 accelerometers. They have been located on main walls near the floor slab in order to detect the global frequency of the palace (Fig. 8). The three external accelerometers (Fig. 9) and the 10 accelerometers located on the third floor of the building are retained in all the configurations tested. In the first configuration (Global Configuration 1) 3 accelerometers were located at the ground floor (+0.0 m), 7 accelerometers at the first floor (+10.5 m), 2 accelerometers at the second floor (+29.5 m) and 9 accelerometers located at the third floor (+34.5 m) (Fig. 6(a)). In the second configuration all the 9 accelerometers are located on the second floor (Fig. 6(b)). In the third configuration all the accelerometers are located around the central staircase (Fig. 6(c)). In the fourth configuration the accelerometers are located in the North

facade (Fig. 6(d)), while in the fifth configuration the accelerometers are located in the South facade (Fig. 6(e)). Multiple tests were repeated at different time of the day for the same configurations and for a duration of 5 minutes each, because the recorded signals were contaminated by the external noise of men working on props interventions of adjacent buildings. The less noised signals were obtained in the late afternoon when props intervention on adjacent buildings terminated. The sampling frequency of each signal is 200 Hz.

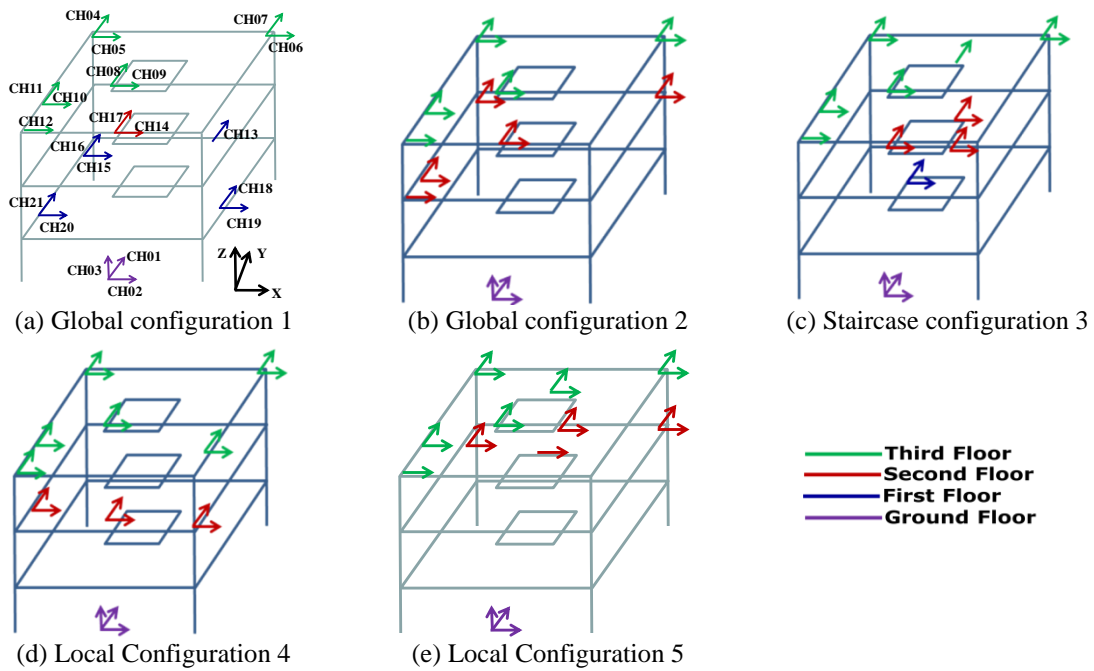


Fig. 6 (a), (b), (c) Location of the acceleration sensors in the global configurations ; (d) in the North Arcade; (e) in the South Arcade



(a)



(b)

Fig. 7 (a) Data acquisition system located at the first floor and (b) cables



Fig. 8 Location of sensors inside the building



Fig. 9 External accelerometers located at the base of the external facade

## **8. Identification of modal parameters**

### *8.1 Results and discussions*

The palace has been severely damaged from the earthquake and the structure itself is very complex, therefore the main natural modes were more difficult to identify. However, removing the signals obtained by sensors located in damage zones where local modes were excited, it was

possible to identify the frequencies of the first three bending modes in the x and y directions. The sampling frequency of each test is 200 Hz, while in configuration 2 is 400 Hz, therefore the plot of the singular value spectrum can be up to a frequency of 100 Hz (Nyquist's frequency). However, the plot in Fig. 11 has been displayed up to a frequency of 16 Hz, because the natural frequencies of the case study are located in the low frequency range. For all the configurations, first the Singular Value Decomposition of the PSD matrixes has been applied following the procedure proposed by Brincker (Brincker *et al.* 2000). Peaks from the plot of the singular value spectrum have been selected and the respective modal frequencies and eigenvectors are identified. The identified frequencies and damping values have been summarized in Tables 1 and 2. The first identified mode shape in the two principal directions have almost the same shape and frequency, because of the symmetric square plan of the palace (Fig. 3), but there are some evidences showing the torsional movements.

The recorded signals in the different configurations due to the symmetry in geometry are considered reliable, as shown by the high values of the MAC coefficient, and this allowed identifying also the second and third mode in the global configuration 2 (Table 2). The frequencies obtained with the three algorithms are very similar with a first bending mode that has a period of 0.38 sec. in the x direction and 0.36 sec. in the y direction (Table 1). The damping ratio varies from 1.69% using the sensors oriented along the x direction to 3.29% using the sensors oriented along the y direction.

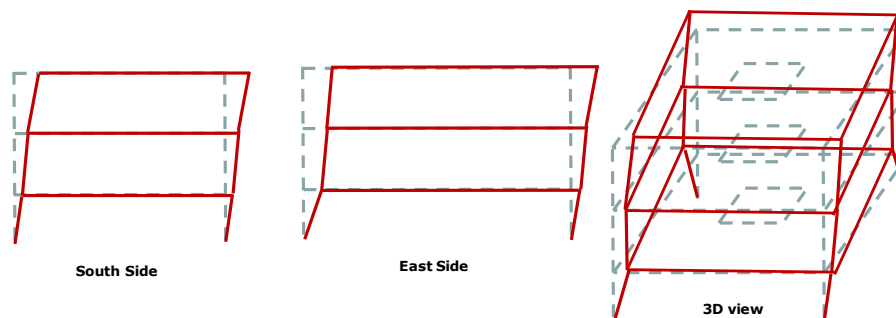


Fig. 10 1<sup>st</sup> identified modal shape of the Palace

Table 1 Identified frequency and damping of the first mode of the Mirandola Town Hall

Alg.		1 <sup>st</sup> Mode (Configuration 1)				1 <sup>st</sup> Mode (staircase configuration 3)			
		Freq. (Hz)	Period (sec)	Damp. (%)	MAC	Freq. (Hz)	Period (sec)	Damp. (%)	MAC
FDD	X dir.	2.66	0.38	-	-	2.73	0.37	-	-
	Y dir.	2.77	0.36	-	-	2.77	0.36	-	-
RD	X dir.	2.64	0.38	-	-	2.64	0.38	-	-
	Y dir.	2.73	0.36	-	-	2.78	0.36	-	-
NExT/	X dir.	2.71	0.37	2.71	95.0	2.68	0.37	1.69	93.4
ERA	Y dir.	2.66	0.38	1.41	80.0	2.75	0.36	3.29	95.5

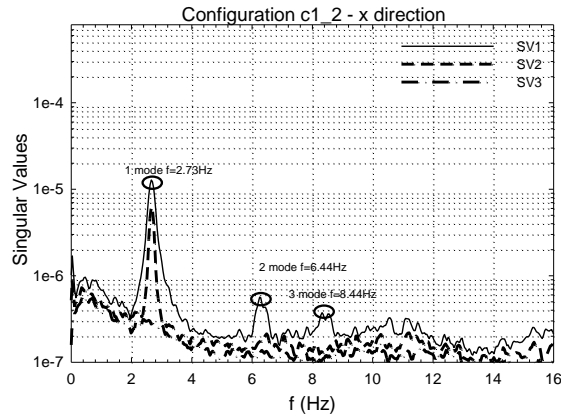


Fig. 11 Singular value of the Town Hall in the X direction using Configuration 1

Table 2 Identified frequencies and damping of the first three modes of the Mirandola Town Hall using Configuration 2

Alg.		1 <sup>st</sup> Mode (Bending X dir.)				2 <sup>nd</sup> Mode (Bending X dir.)				3 <sup>rd</sup> Mode (Bending X dir.)			
		Freq. (Hz)	Period (sec)	Damp. (%)	MAC	Freq. (Hz)	Period (sec)	Damp. (%)	MAC	Freq. (Hz)	Period (sec)	Damp. (%)	MAC
FD	X dir.	2.66	0.38	-	-	6.25	0.16	-	-				
D	Y dir.	2.73	0.37	-	-	6.88	0.15	-	-				
RD	X dir.	2.64	0.38	-	-	6.05	0.17	-	-	9.96	0.10	-	-
	Y dir.	2.83	0.35	-	-	6.84	0.15	-	-	9.86	0.10	-	-
NEx T/	X dir.	2.66	0.38	4.23	83.7	6.06	0.17	4.4	50.3	10.3	0.10	2.78	63.3
										13.2	0.08	1.61	54.5
ER	Y dir.	2.75	0.36	4.11	90.3	7.27	0.14	0.14	62.7	4			
A													

The MAC coefficient is quite high, indicating that the results are reliable for both groups. When considering the second mode, the natural frequencies identified with the three algorithms are in good agreement with the sensors oriented in the x direction where difference of 4% can be observed among the algorithms, while differences of 13% are observed when considering sensors oriented in the y direction. The second bending mode (Table 2) has a period of about 0.04 sec using the sensors oriented along the x and y direction. Furthermore in the both directions a damping ratio of 0.3% is obtained. For completeness, the third mode has a period of 0.03 sec (Table 2), while the damping ratio and the MAC coefficient are given in Table 2.

### 8.2 Correlation coefficient

The correlation coefficients among the various signals' channels and the ground input signal have been evaluated for the three configurations. Distinction has been made between x and y direction (Table 3). What can be observed is that where the correlation is low and close to zero probably the level of damage inside the building is higher, because probably macro elements of the structure are not anymore connected to the main body of the building. In particular according to the analysis of the correlation coefficient of the configuration 2 the South East and South West

corner of the building are less correlated as marked in the gray area in Table 3. This result is confirmed by on site observations because the South facade (Fig. 12) had the local collapse of the South Vault shown in Fig. 3 and highlighted in Fig. 14. In the same figure structural damage is also located in the North West corner of the building which corresponds to the area that was stiffened with the scaffolding s shown in Fig. 13.

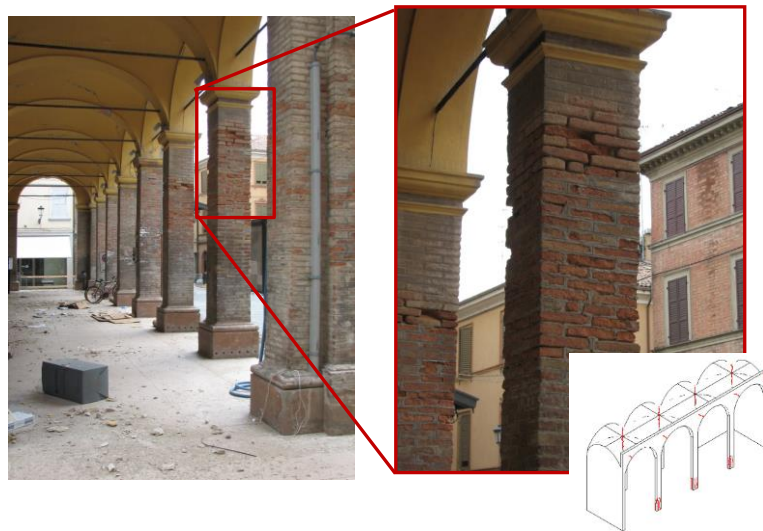


Fig. 12 Damage to the columns of the Arcades of the South Facade



Fig. 13 Scaffolding in the North-West side of the Facade during May 29<sup>th</sup> Shock

Table 3 Correlation coefficients among the various channels in x and y direction

Configuration 1				Configuration 2				Staircase configuration 3			
Ch. X Dir.	$\rho_x$	Ch. Y Dir.	$\rho_y$	Ch. X Dir.	$\rho_x$	Ch. Y Dir.	$\rho_y$	Ch. X Dir.	$\rho_x$	Ch. Y Dir.	$\rho_y$
15	0.005	16	0.001	6	0.013	11	0.002	9	0.003	21	0.042
9	0.012	8	0.020	19	0.013	16	0.004	20	0.012	16	0.054
6	0.024	4	0.024	20	0.014	18	0.005	15	0.018	4	0.062
14	0.025	11	0.027	13	0.057	17	0.007	5	0.041	7	0.075
19	0.042	17	0.031	10	0.064	4	0.008	12	0.044	13	0.077
5	0.064	21	0.046	12	0.071	8	0.009	14	0.049	8	0.083
12	0.072	7	0.053	5	0.085	21	0.040	10	0.071	17	0.092
20	0.074	18	0.054	15	0.090	7	0.044	6	0.071	18	0.112
10	0.080	13	0.134	9	0.092	1	1.000	19	0.078	11	0.150
2	1.000	1	1.000	14	0.167	2	1.000	2	1.000	1	1.000
				2	1.000						

Furthermore by comparing the Fast Fourier Transform of the signals of channels 4 and 7 oriented in the North-South direction, it can be observed that the PSD of the signal of channel 7 is able to identify also the second mode of the building, which cannot be observed in the PSD of channel 4. This is probably justified by the fact that this channel is also close to one of the most damage parts of the building. This is the same reason why in the staircase configuration 3 the only channel which is able to determine the second mode by using the FFT is the channel 11 which is located in the North West corner of the building which had less damage by field observations.

In the third configuration shown in Fig. 15 (staircase configuration 3) the correlation is very low in all the channels because they were located around the stairs which resulted extensively damaged after the earthquake.

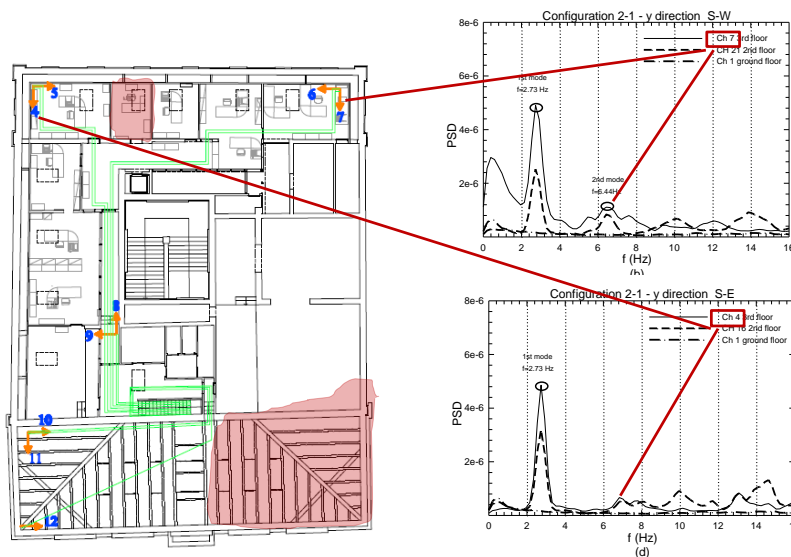


Fig. 14 Frequencies identified with Global Configuration 2 using FFT

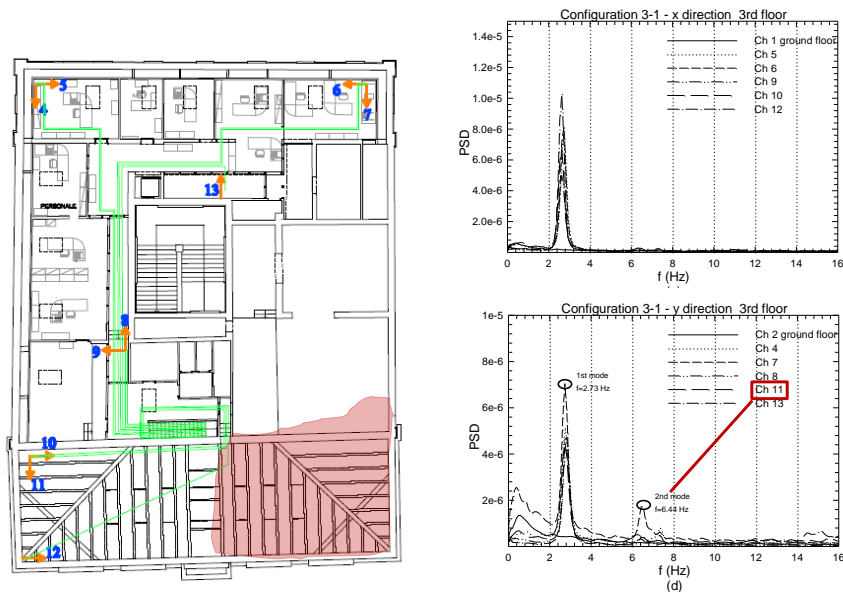


Fig. 15 Frequencies identified with staircase configuration 3 using FFT

## 9. Conclusions

Dynamic characteristics such as the natural frequencies, the mode shapes, and the damping ratios of Mirandola Town Hall, an historical monumental palace which was damaged during 2012 Emilia earthquake, were determined using ambient vibration data. Three output-only modal identification techniques have been used: (i) the Frequency Domain Decomposition, (ii) the Random Decrement (RD) and the (iii) Eigensystem Realization Algorithm (ERA). Measurements were made in the Palace with five different configurations using 21 sensors and the ambient vibration tests involved the simultaneous measurements of longitudinal and lateral vibrations. Good modal identification of the lateral vibration modes was achieved for the Palace, in fact a total of 3 modal frequencies and modal displacement shapes were identified, that are in the frequency range 0 to 35 Hz. The comparison of the three experimental techniques shows a good agreement confirming the reliability of the three identification methods, even though the NeXT-ERA method provides additional parameters such as the damping ratio and the MAC index that is an indicator of the reliability of the results.

## Acknowledgements

The research leading to these results has received funding from the European Community's Seventh Framework Programme - Marie Curie International Reintegration Actions - FP7/2007-2013 under the Grant Agreement n° PIRG06-GA-2009-256316 of the project ICRED - Integrated European Disaster Community Resilience.

## References

- Abdel-Ghaffar, A.M. and Scanlan, R.H. (1985), "Ambient vibration studies of Golden Gate Bridge: II. pier-tower structure", *J. Eng. Mech. - ASCE*, **111**(4), 483-499.
- Bendat, J.S. and Piersol, A.G. (2000), *Random data: analysis and measurement procedures*, Wiley, New York.
- Brincker, R., Zhang, L. and Andersen, P. (2000), "Modal identification from ambient responses using frequency domain decomposition", *Proceedings of the International Modal Analysis Conference (IMAC)*, San Antonio, Texas.
- Caicedo, J.M., Dyke, S.J. and Johnson, A.E. (2004), "Natural excitation technique and eigensystem realization algorithm for phase i of the iasc-asce benchmark problem: simulated data", *J. Eng. Mech. - ASCE*, **130**(1), 49-60.
- Chang, C.C., Chang, T.Y.P. and Zhang, Q.W. (2001), "Ambient vibration of long-span cable-stayed bridge", *J. Bridge Eng.*, **6**(1), 46-53.
- Cimellaro, G.P., Chiriatti, M., Reinhorn, A.M. and Tirca, L. (2012), *Emilia Earthquake of May 20th, 2012 in Northern Italy: rebuilding a resilient community to multiple hazards*, MCEER Technical Report –MCEER-12-0009, MCEER, State University of New York at Buffalo (SUNY), Buffalo, New York.
- Cimellaro, G.P., Piantà, S. and De Stefano, A. (2012), "Output-only modal identification of ancient L'Aquila City Hall and Civic Tower", *J. Struct. Eng. - ASCE*, **138**(4), 481-491.
- Cimellaro, G. P. and Reinhorn, A.M. (2011), "Multidimensional performance limit state for hazard fragility functions", *J. Eng. Mech. - ASCE*, **137**(1), 47-60.
- Cole, H.A. (1968), "On-the-line analysis of random vibrations", *AIAA Paper*, 68-288.
- James, G.H., Carne, T.G. and Lauffer, J.P. (1993), *The natural excitation technique for modal parameter extraction from operating wind turbines*, Sandia National Laboratories.
- James, G.H., Carne, T.G. and Mayes, R.L. (1996), "Modal parameter extraction from large operating structures using ambient excitation", *Proceedings of the 14th Int. Modal Analysis Conf., Dearborn, Michigan, USA*.
- Juang, J.N., Cooper, J.E. and Wright, J.R. (1988), "An eigensystem realization algorithm using data correlations (ERA/DC) for modal parameter identification", *Control Theory Adv. Technol.*, **4**(1), 5-14.
- Juang, J.N. and Pappa, R.S. (1986), "Effect of noise on modal parameters identified by the eigensystem realization algorithm", *J. Guid. Control Dynam.*, **9**(3), 294-303.
- Juang, J.N. and Pappa, R.S. (1985), "An eigensystem realization algorithm for modal parameter identification and model reduction", *J. Guid. Control Dynam.*, **8**(5), 620-627.
- Nagayama, T., Abe, M., Fujino, Y. and Ikeda, K. (2005), "Structural identification of a nonproportionally damped system and its application to a full-scale suspension bridge", *J. Struct. Eng. -ASCE*, **131**(10), 1536-1545.
- Piantà, S., Cimellaro, G.P. and De Stefano, A (2011), "Experimental and numerical modal identification of L'Aquila Margherita Palace", *Proceedings of the SMAR 2011, First Middle East Conference on Smart Monitoring, Assessment and Rehabilitation of Civil Structures (SMAR 2011)*, American University in Dubai (AUD), Dubai UAE, 8 –10 February.
- Saudi, G., Reynolds, P., Zaki, M. and Hodhod, H. (2009), "Finite-element model tuning of global modes of a grandstand structure using ambient vibration testing", *J. Perform. Constr. Fac.*, **23**(6), 467-479.